ELSEVIER

Polymer 40 (1999) 513–518

polymer

Morphology variation as a function of composition for blends of PVDF and a polyaniline derivative

L. H. C. Mattoso[a,*], L. F. Malmonge[1b]

[a]*Centro Nacional de Pesquisa e Desenvolvimento de Instrumentação Agropecuária, CNPDIA/EMBRAPA, C.P. 741, São Carlos, 13560-970, SP, Brazil*
[b]*Instituto de Química de São Carlos, USP, C.P. 369, São Carlos, 13560-970, SP, Brazil*

Received 11 February 1998; accepted 30 March 1998

Abstract

Blends of poly(vinylidene fluoride), PVDF, and poly(*o*-methoxyaniline), POMA doped with toluene sulfonic acid, TSA, were prepared by casting at various compositions and studied by scanning electron microscopy, X-ray diffraction and differential scanning calorimetry. The blend composition has a great influence on the morphology obtained. As the concentration of POMA–TSA is increased in the blend an interconnecting fibrillar-like morphology is formed and the spherulites characteristic of pure PVDF are destroyed. The variation of blend morphology is further discussed based on X-ray diffraction and differential scanning calorimetry analysis.

Keywords: Conducting polymers; Polyanilines; Blends

1. Introduction

The possibility of processing conducting polymers in the form of blends with commercial polymers [1] has opened a wide range of applications and increased the technological potential of these materials since some properties of these two classes of polymers can be combined in a synergistic matter. Polyaniline, PANI, for instance, may be blended with a variety of polymers [1–6] such as polyethylene, polypropylene, polystyrene, poly (methylmethacrylate), nylon, styrene–butadiene block copolymers, etc.

Despite the great number of blends that have been prepared in the last few years [1–7], there is still little work done on the characterization of the morphology and structure of these materials. It is well known in polymer science that the morphology and phase distribution is important to understand the relationship between structure and properties, as well as to predict properties or even to design new materials with specific characteristics. In the conducting polymer field, and more specifically in blends of PANI and PMMA [8], it has been shown that the extremely low percolation threshold is due to an unusual morphology, where the doped polyaniline forms conductive pathways within the matrix. Such morphology greatly contributes for the high conductivity values obtained.

The aim of the present work is to study the influence of blend composition on the morphology and structure of poly(*o*-methoxyaniline) and PVDF blends, as studied by scanning electron microscopy, X-ray diffraction and differential scanning calorimetry.

2. Experimental

2.1. Polymer synthesis

Poly(*o*-methoxyaniline) (POMA) was chemically synthesized with ammonium peroxydisulphate in aqueous 1.0 M HCl at 0°C, as described elsewhere [9,10]. Deprotonation was performed with 0.1 M ammonium hydroxide for 16 h at room temperature to yield the polymer in the emeraldine base form. The resulting polymer was then dried under dynamic vacuum for 24 h at room temperature. Poly (vinylidene fluoride) (PVDF), Foraflon 4000 HD, was purchased from Atochem and used as received.

2.2. Preparation of blends

Stock solutions of the conducting polymer (2% weight/volume) and PVDF (10% w/v) in dimethylacetamide

* Corresponding author.
[1] Also at Depto Física e Química, UNESP, Ilha Solteira, 15385-000, SP, Brazil.

0032-3861/98/$ - see front matter
PII: S0032-3861(98)00280-8

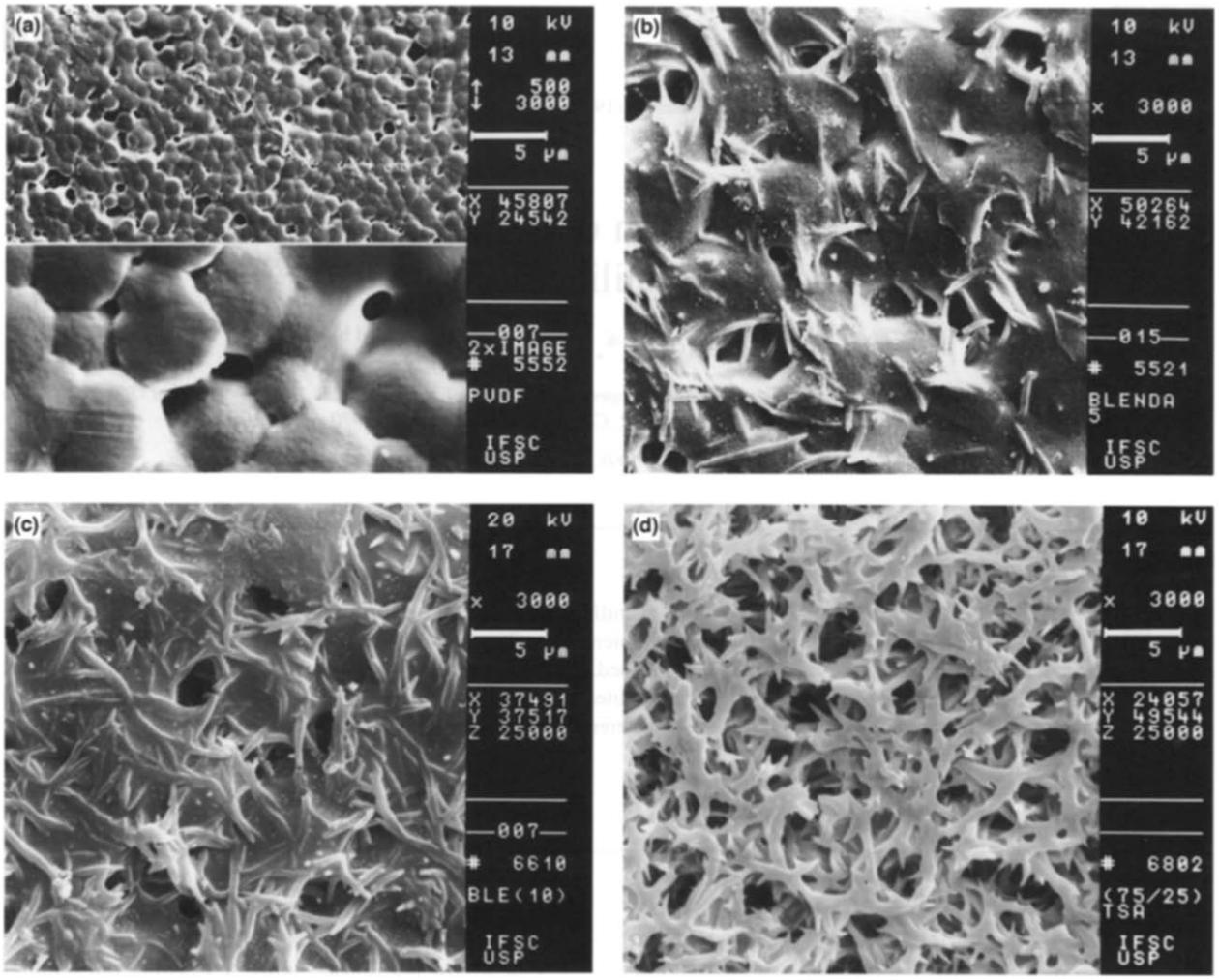

Fig. 1. Scanning electron microscopy images of PVDF/POMA–TSA blends with the following compositions: (a) 100/0; (b) 95/5; (c) 90/10; (d) 75/25.

(DMA) were prepared separately. For the preparation of doped POMA blends, protonic doping of POMA-EB dissolved in DMA was carried out by addition of toluene sulfonic acid (TSA) in order to have a 50% doping level. No detectable insoluble fraction was noticed upon filtering the solutions. Films (15–30 μm thick) were prepared by casting the blend solutions, mixed at various composition (PVDF/POMA = 100/0, 99/1, 95/5, 90/10, 75/25, 50/50, 30/70, 10/90, 0/100), on a pre-heated glass slide, placed in an oven (50°C) with air circulation. Solvent evaporation was complete after ca. 1 h at 50°C.

2.3. Characterization

Scanning electron microscopy (SEM) was perfomed in a ZEISS DSM 960 computorized microscope operated between 10 and 20 kV on samples containing a thin layer (ca. 15 nm) of gold sputter coated. Electrical conductivities were measured by the standard four-probe method. X-ray diffraction patterns were taken on a Rigaku RU-200B diffractometer, using Cu K-a radiation and a Ni filter. Thermal analysis was done in a differential scanning calorimetry (DSC) Du pont model 2000 at a scan rate of 10°C/min in nitrogen atmosphere.

3. Results and discussion

In the present study the morphology and structure of blends with different compositions of PVDF and POMA doped with TSA were investigated. From Fig. 1 one can observe that the morphology of the blends, prepared in the same conditions, changes upon POMA content increase. PVDF micrograph (Fig. 1*a*) consists of spherical patterns characteristic of a spherulitic morphology, as investigated by SEM. Such morphology formed by small spherulites of diameter of about 6 μm is consistent with the literature [11], for PVDF crystallized at low temperatures (below 100°C) where the spherulites nucleation rate are high but the growth rate are usually low. Although its size and shape can change with film preparation conditions, the spherulites are usually always present [11,12].

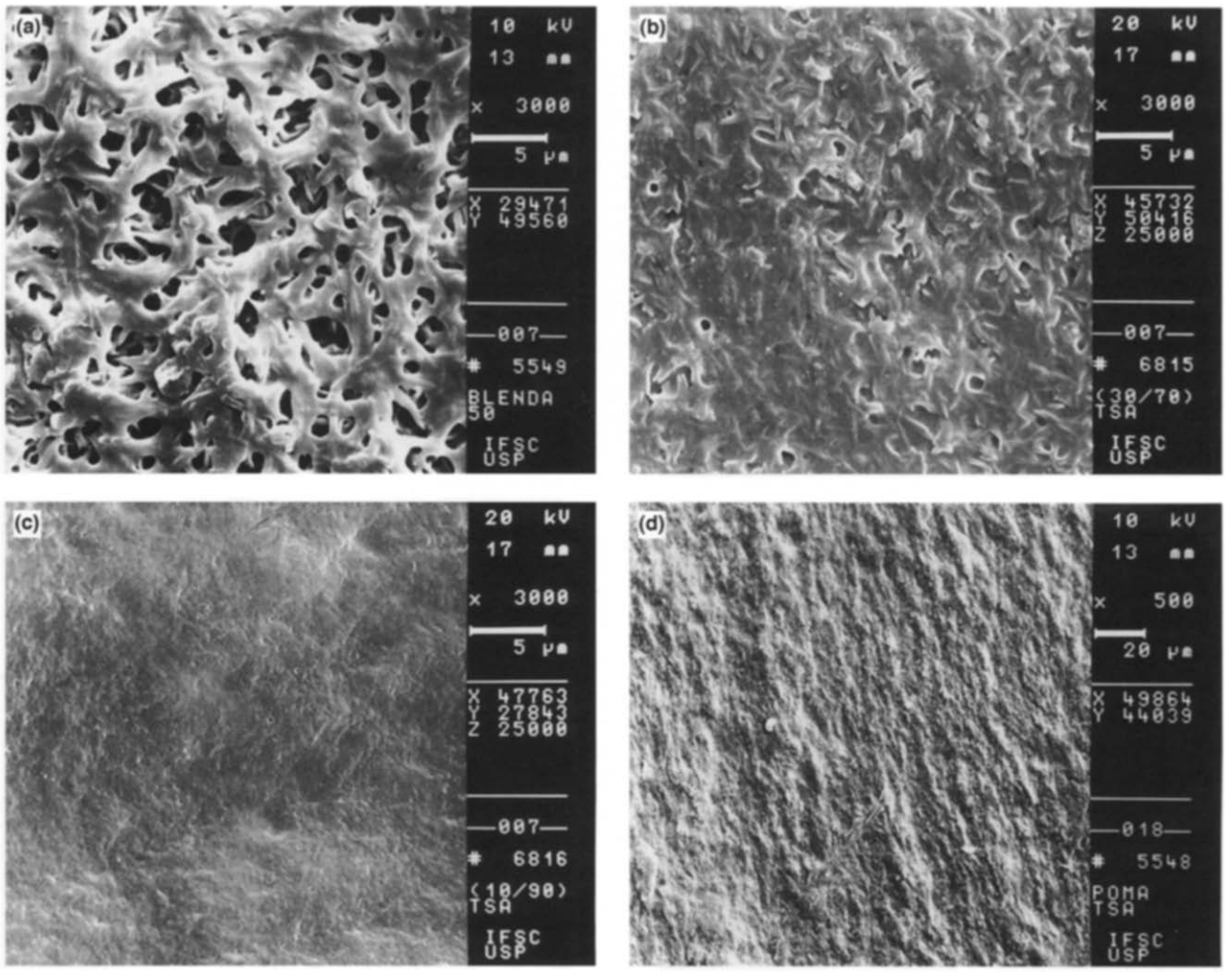

Fig. 2. Scanning electron microscopy images of PVDF/POMA–TSA blends with the following compositions: (a) 50/50; (b) 30/70; (c) 10/90 and (d) 0/100.

Interestingly, the addition of POMA doped with TSA has a great influence on the spherulitic morphology observed for pure PVDF. Starting for blends with low POMA–TSA contents (5%) the morphology presented the growth of fibrils in the form of straight rods of ca. 350 nm of diameter and as long as 7 μm (Fig. 1*b*). Such fibrils seem to be located preferentially in the boundaries of the spherulites. As one increase the POMA content for 10% (Fig. 1*c*), such fibrils are already spread all over the polymer blend surface, whose spherulitical pattern can be hardly noted, but a background continuous matrix. The fibril diameter basically did not change, but the fibril size seems to be increased, starting to show some interconnecting behavior. For blends containing 25% of POMA–TSA (Fig. 1*d*) the spherulites features can not be seen at all, the morphology consisting predominantly of interconnected fibrils of diameter around 700 nm, which are throughout the entire surface of the blend with a more porous opened structure.

As the amount of POMA–TSA in the blend increases to 50% the diameter of the fibrils increases and the porous size decreases (Fig. 2*a*). Apparently, the fibrils are coalescing into each other. For even greater amounts of POMA–TSA (70–90%) the porous have almost disappeared as well as the fibrils feature, the morphology being so closed and compacted that the fibrils seems to have completely coalesced (Fig. 2*b*, *c*). Such compact morphology is consistent with that observed for pure POMA–TSA as can be seen in Fig. 2*d*.

To evaluate if the bulk morphology of the blend would also have a similar fibrillar-like pattern the blend PVDF/POMA TSA 75/25 was broken in liquid nitrogen and its cross-section analyzed by scanning electron microscopy. Fig. 3*a*, *b* shows that, as expected, a fibrillar-like pattern is also seen in the volume of the blend whose fibril density apparently changes along the film thickness, probably due to the solvent evaporation gradient during the film formation by casting.

It should be pointed out that in other studies it has been detected that PANI [13,14], as well as its derivatives such as POMA [9], usually possess a fibrillar morphology whose diameter can vary in the range from 100 to 700 nm depending on the preparation conditions used. It is interesting to observe that other types of morphologies with globular or lamelar shape can be also obtained depending mainly on the dopant used, specially for polyanilines prepared by electrodeposition [15,16].

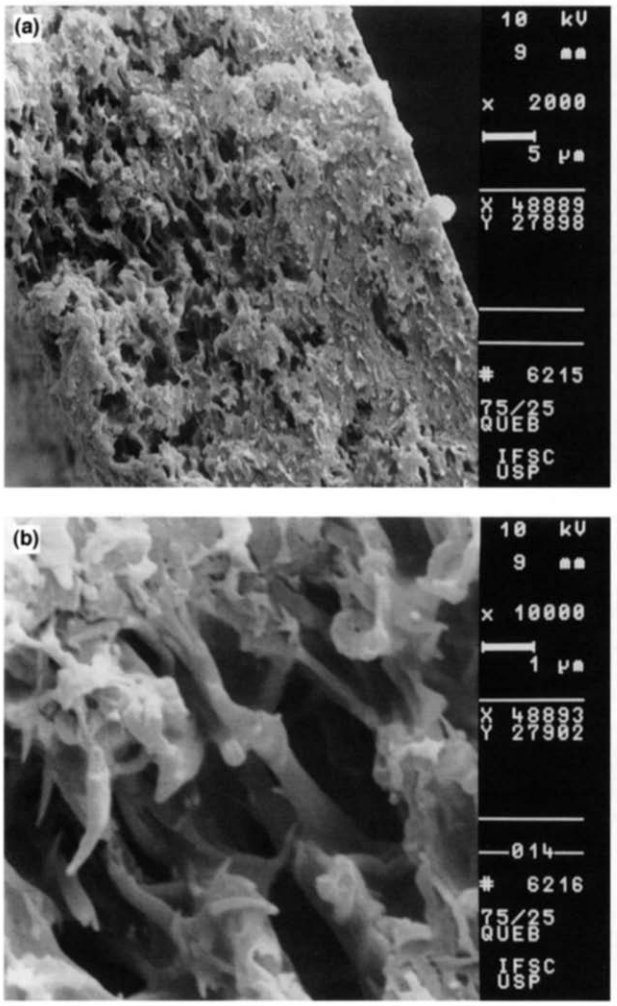

Fig. 3. Scanning electron microscopy images of the cross section of PVDF/POMA–TSA (75/25) blends broken in liquid nitrogen. Magnification: (a) 2000×; (b) 10 000×.

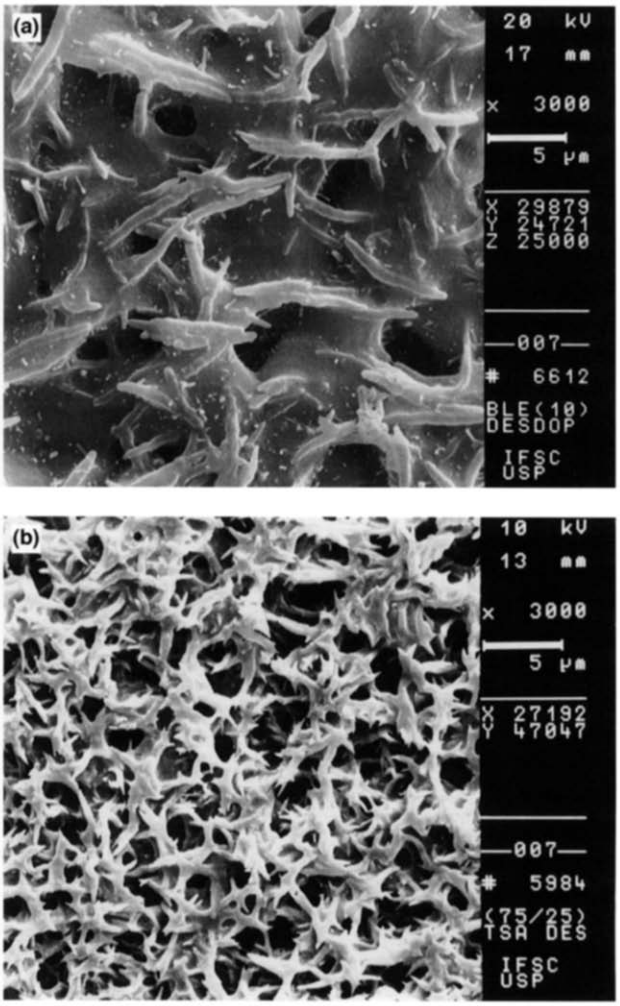

Fig. 4. Scanning electron microscopy images of PVDF/POMA–TSA (75/25) blends dedoped in NH_4OH 0.1 M (80 h). Blend compositions: (a) 90/10 and (b) 75/25.

In order to investigate the origin of the fibrils within the blend two compositions were analyzed, namely PVDF/POMA–TSA 75/25 and 90/10. Firstly, these samples were dedoped to eliminate the possibility that the dopant could be forming such fibrils itself. This is particularly important to check, since at room temperature TSA is at the solid state, which could be not only doping POMA, but also segregating in the form of fibrils. However, the same fibrillar morphology obtained for the original untreated blend is still obtained for the dedoped blends, as it can be seen in Fig. 4*a*, *b*. The complete dopant removal is confirmed by the conductivity decay of these samples, which decreased to the values characteristic of dedoped POMA (below 10^{-7} S/cm) and also by the colour change from green (wavelength maximum of ca. 850 nm in the u.v.–vis analysis) to blue (ca. 600 nm) characteristic of the transition from the doped to the dedoped state of the polymer, in agreement with the literature [17–20].

Subsequently, the dedoped blends samples were then treated with *m*-cresol in order to extract the POMA component in the blend and analyzed by SEM. Fig. 5*a*, *b* shows that the resulting morphology comprises a PVDF matrix with voids corresponding to the exact shape of the so-called POMA fibrils, which were removed by the extraction treatment. The POMA extraction is further evidenced by the colour change from dark blue to a colourless transparent film upon extraction, characteristic of pure PVDF. These observations corroborate other studies [8] showing the formation of an interconnected morphology, which is of key importance for obtaining conductive blends with low percolation threshold. Indeed, we have demonstrated in previous work [10,21] that these types of blends do present a low percolation threshold which is below 5%, for instance, reaching conductivity of about 10^{-5} S/cm for POMA–TSA content of 4.5% in the blend.

The X-ray analysis confirms the presence of a crystalline phase within the blends. From Fig. 6 one can see that the crystalline peaks characteristic of β-PVDF [12,22] at ca. $\theta = 20°$ are maintained in the blend, besides the presence of the POMA component, which at least for low contents (below 25%) does not affect the β-PVDF structure.

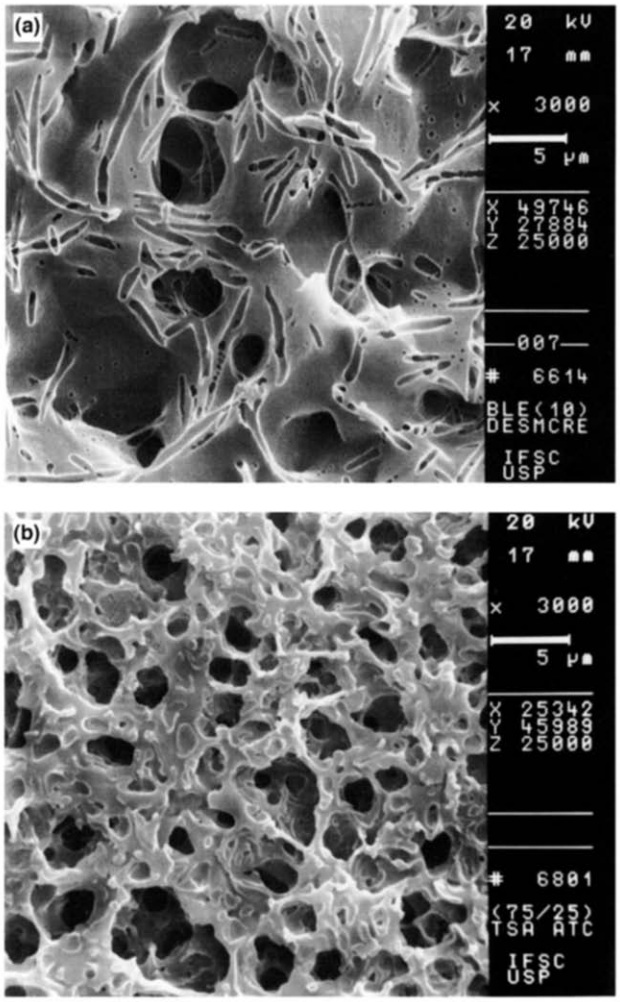

Fig. 5. Scanning electron microscopy images of PVDF/POMA–TSA (75/25) blends dedoped in NH_4OH 0.1 M (8 0h) and then extracted with *m*-cresol. Blend compositions: (a) 90/10 and (b) 75/25.

Apparently, POMA is located initially at the amorphous PVDF phase and/or between the spherulites. This is also supported by evidence of SEM analysis (Fig. 1*b*) which showed an indication of fibrils at the boundaries for 5% of POMA in the blend. The growth of an ordered structure with peaks at ca. $2\theta = 7.5°$ can be observed for POMA contents above 25%. Also, less intense and broader peaks appears in the range of 2θ from 25° to 27° and for 2θ from 13° to 18°. Although these peaks are in about the same range as those obtained for α-phase PVDF ($2\theta = 17.5°$, 18.4°, 20°, 26°) [12,22], we observe that for higher POMA contents the main crystalline diffraction peak of PVDF at ca. $2\theta = 20°$ completely disappears, indicating destruction of the PVDF crystalline phase. Furthermore, this behaviour is accompanied by the increase on the intensity of peaks at 7.5° 13°, 23° and 27°, which are assigned for ordered regions in POMA–TSA (Fig. 6). Such ordered structure in polyanilines has been associated with the presence of the dopant, which has been reported [23,24] to favour crystallization. Considering these previous results, it was interesting to note that in our

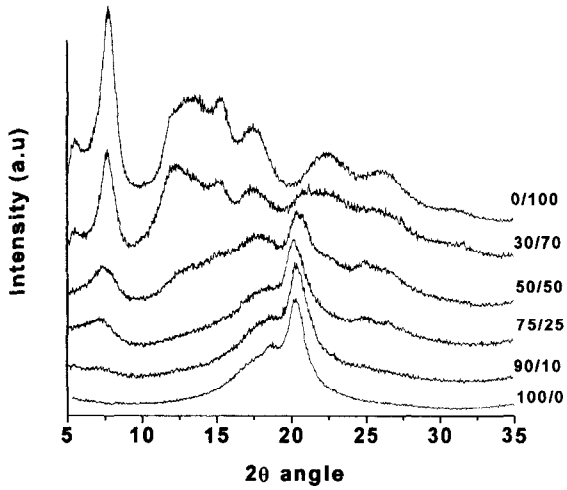

Fig. 6. X-ray diffraction patterns of PVDF/POMA–TSA blends with different compositions, as indicated.

case the diffraction pattern of the blend does not change upon dedoping the blend. This indicates that the ordered POMA structure is maintained in the blend even dedoping the polymer after blend preparation.

Comparing the SEM and X-ray data we note that the PVDF spherulites seem to disappear at composition from 10 to 25% of POMA–TSA, whereas for the X-ray the PVDF crystalline peaks disappear at the composition from 50% to 70% of POMA–TSA. Actually at 70% of POMA content there may still exist some remaining contribution from the diffraction peak of PVDF which is apparently covered by the shoulder of the POMA peak at ca. $2\theta = 23°$. A possible explanation for the differences between SEM and X-ray data is that SEM analysis indicates the morphology of the crystalline structure of PVDF at a larger scale (spherulite scale) in the range of 5 μm, whereas the X-ray can detect crystallinity within the crystal lamellae (Angstrom scale), which forms the spherulites. Therefore, upon POMA addition the crystalline structure of PVDF is affected in two steps: first on the spherulites for POMA contents from 10 to 25% and then on the crystalline lamellae for POMA contents from around 70%.

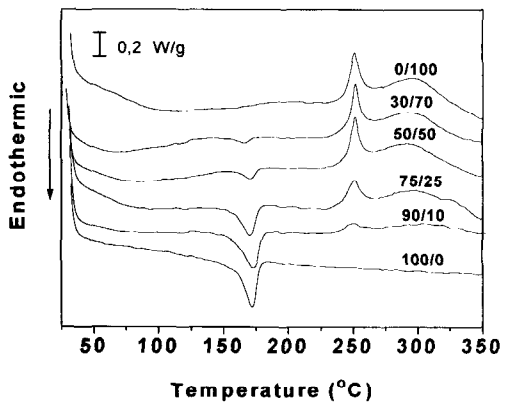

Fig. 7. Differential scanning calorimetry thermograms of PVDF/POMA–TSA blends with different compositions, as indicated.

Such hypothesis is corroborated by DSC data shown in Fig. 7. One observes that the endothermic fusion peak at 170°C characteristic of PVDF [12,25] is observed for blend composition up to 50–70% of POMA–TSA, consistent with the presence of remaining crystalline crystals of PVDF. Obviously, the enthalpy of fusion decreases with the decrease of PVDF content within the blend, as expected. No endothermic fusion peak is observed for POMA–TSA, but an exothermic peak at around 240°C. Such peak is associated with the degradation of polyanilines and occurs before any fusion peak can be observed, in agreement with the literature [26,27].

4. Conclusions

The composition of PVDF/POMA blends has a great influence on the morphology of the films obtained. As the concentration of POMA–TSA is increased in the blend a interconnecting fibrillar-like morphology is formed whereas spherulites of about 5 μm in diameter, characteristic of pure PVDF, are destroyed. The X-ray analysis confirms the presence of the β-crystalline phase characteristic of PVDF within the blends, besides the presence of the POMA component, which at least for low contents (below 25%) do not affect the β-PVDF structure. The growth of an ordered structure with main peak at ca. $2\theta = 7.5°$ can be observed for POMA contents above 25%. Furthermore, the endothermic fusion peak characteristic of PVDF is observed for blend composition up to 50–70% of POMA–TSA, consistent with the presence of crystalline crystals of PVDF. These results suggest that the crystalline structure of PVDF is affected, upon POMA addition, in two steps: first on the spherulites for POMA contents from 10% to 25% and then on the crystalline lamellae for POMA contents from around 70%.

Acknowledgements

The financial support given by FAPESP, CAPES and CNPq (Brazil) is gratefully acknowledged.

References

[1] Cao Y, Smith P, Heeger AJ. Synth Met 1993;32:263.
[2] Virtaen E, Laakso J, Ruohonen H, Vakiparta K, Jarvinen H, Jussila M, Passiniemi P, Osterholm J-E. Synth Met 1997;84:113.
[3] Laska J, Zak K, Pron A. Synth Met 1997;84:117.
[4] Fu Y, Weiss RA. Synth Met 1997;84:103.
[5] Davies SJ, Ryan TG, Wilde CJ, Beyer G. Synth Met 1995;69:209.
[6] Macinnes, D Jr, Contemporary Topics in Polymer Science, Vol. 7, ed. JC Salamone, J Riffle. Plenum Press, New York, 1992.
[7] Mammone RJ, Wade WL Jr, Binder M. Proceedings of the 25th Intersociety Energy Conversion Engineering Conference, Nevada, 3 August 1990, p. 385.
[8] Yang CY, Cao Y, Smith P, Heeger AJ. Synth Met 1993;53:293.
[9] Mattoso LHC, Faria RM, Bulhoes LOS, MacDiarmid AG. Polymer 1994;35:5104.
[10] Malmonge LF, Mattoso LHC. Polymer 1995;36:245.
[11] Gregório R Jr, Cestari MJ. Polym Sci Part A: Polym Phys 1994;32:859.
[12] Gregório R Jr, Cestari M, Nociti NCPS, Mendonça JA, Lucas AA. In: The Encyclopedia of Polymeric Material, ed. JC Salamone. CRC Press, Boca Raton, FL, 1996, p. 7128.
[13] Wei Y, Sun Y, Jang G-W, Tang X. J Polym Sci: Part C: Polym Lett 1990;28:81.
[14] Nyffenegger R, Gerber C, Siegenthaler H. Synth Met 1993;55-57:402.
[15] Duic Lj, Mandic Z, Kovacicek F. J Polym Sci Polym Chem 1994;32:105.
[16] Motheo AJ, Santos JR Jr, Venancio EC, Mattoso LHC. Polymer 1998 (in press).
[17] Call RP, Grinder JM, Leng JM, Ye HJ, Manohar SK, Master JG, Asturias GE, MacDiarmid AG, Epstein AJ. Phys Rev B 1990;41:5202.
[18] Huang WS, MacDiarmid AG. Polymer 1993;34:1833.
[19] MacDiarmid AG. Second Brazilian Polymer Conference, São Paulo, 1993, p. 544.
[20] MacDiarmid AG, Epstein AJ. Synth Met 1994;65:103.
[21] Malmonge, LF, Ph.D. Thesis, Universidade de São Paulo, São Carlos, 1996.
[22] Lovinger AJ, Developments in Crystalline Polymers—1, ed. DC Basset. Applied Science, London, 1982.
[23] Pouget JP, Jozefowicz ME, Epstein AJ, Tang X, MacDiarmid AG. Macromolecules 1991;24:779.
[24] Nicolau YF, Djurado D. Synth Met 1993;55-57:394.
[25] Qudaj AMA, Al-Raheil IA. Polym Int 1995;38:381.
[26] Milton AJ, Monkman AP. Synth Met 1993;55:3571.
[27] Wei Y, Jang GW, Hsueh KF, Scherr EM, MacDiarmid AG, Epstein AJ. Polymer 1992;33:314.